ARMA 17-845

Modifications for the Smooth Joint Contact Model in the Particle Flow Code

Mehranpour, M.H. and Kulatilake, P.H.S.W

Rock Mass Modeling and Computational Rock Mechanics Laboratories, The University of Arizona, Tucson, AZ, USA

ABSTRACT: This paper deals with the following two shortcomings of the smooth joint contact model (SJCM) used in the particle flow code (PFC): (a) Use of a constant value for joint normal stiffness instead of allowing actual non-linear behavior between the joint normal deformation and joint normal stress; (b) The so called "interlocking problem". The first one is solved by imposing a linear relation between the joint normal stiffness and the normal contact stress in a new modified smooth-joint contact model (MSJCM). A good agreement obtained between the results from the experimental tests and the numerical modeling of the compression joint normal test, shows the accuracy of this new model. The second shortcoming occurs due to a lack of an updating procedure in the PFC software related to the contact conditions of the particles that lie around the intended joint plane during high shear displacements. This problem increases the shear strength of the joint when the shear displacement of the joint exceeds a specific value and creates unwanted fractures around the intended joint plane. To solve this problem a new approach termed joint side checking (JSC) is proposed. Numerical modeling of the direct shear test shows JSC can solve the interlocking problem and proves to be more consistent with the theory compared to the regular approach.

1. INTRODUCTION

Nowadays, through the development of commercially available Distinct Element Method (DEM) software packages on one hand and accessibility to extremely fast computers on the other hand, DEM has become popular in geomechanics (Cundall, 1971 & 1980; Cundall Strack, 1979; Cundall 1988; Itasca, 2016; Kulatilake et al., 1993; Wu and Kulatilake 2012; Kulatilake and Biao, 2015; Shreedharan and Kulatilake 2016). DEM is a discontinuum mechanics based method in which material is modeled by rigid or deformable blocks/particles, and Newton's second law acts between blocks/particles. The Particle Flow Code (PFC) as a DEM software package uses rigid disks and spherical elements to represent particles in 2D and 3D, respectively. Since PFC can properly model the fracture initiation and propagation between particles by Bonded-Particle Models (BPMs) as well as sliding along joints by Smooth-Joint Contact Model (SJCM), it is a powerful technique to model jointed rock masses (Potyondy and Cundall, 2004; Mas Ivars, 2011; Potyondy, 2015).

In the Bonded-Particle Models (BPMs) adjacent particles adhere together at their contacts to represent the intact rock. The Linear Contact Bond Model (LCBM), the Linear Parallel Bond Model (LPBM) and the Flat-Joint Contact Model (FJCM) are three common BPMs. Each contact in BPMs has two modes: bonded and unbonded. At the time of particle assembly, two adjacent particles bond together at their contact; this contact is in the bonded mode. Then during the model execution, if the bonded contact breaks due to its strength limit in shear or tension, the bonded mode changes to unbonded mode. The Linear Contact Model (LCM) is the common unbonded contact model in BPMs. Besides, if two particles were not connected at the time of particle assembly but they connect each other during the model execution, this new contact is also a linear contact. The LCM provides the linear elastic behavior in the normal and shear directions in which the shear strength is limited by imposing the Coulomb criteria, compressive strength is unlimited and tension strength is zero (Potyondy, 2015).

In BPMs, since particles are rigid, displacements only occur at the contacts through the penetration, sliding and rotation of particles around each other (Itasca, 2016). In BPMs, on one hand, sliding occurs at the particle perimeters and on the other hand the shear direction is always perpendicular to the line which connects the centers of the two particles (which is called the "line connecting the centers" in the rest of the paper). Therefore, it is difficult to apply a joint with a specific direction in BPMs and this joint contains an inherent

dilation angle which increases the friction coefficient of the joint.

In order to solve the aforementioned problems, the SJCM was proposed (Potyondy and Cundall, 2004; Mas Ivars, 2011; Potyondy, 2015). In the SJCM, two particles can slide on each other by crossing each other along a hypothetical joint plane which is parallel to the intended joint plane and is located at the midway between the centers of the two particles (Fig. 1). Consequently, SJCM can model a joint with any direction (Mas Ivars, 2011).

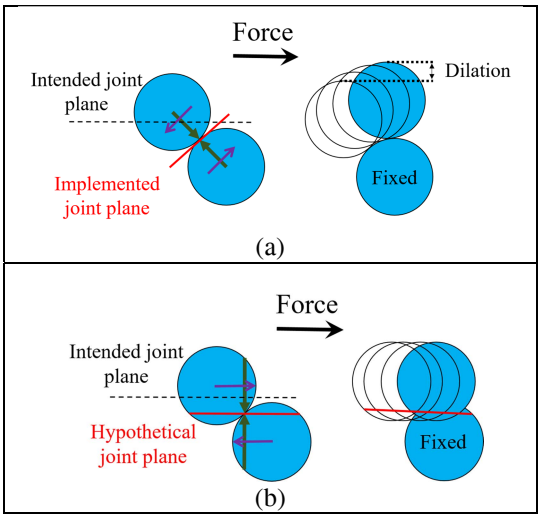

Fig. 1. Force components, and particle motion of (a) the linear contact model, and (b) the smooth-joint contact model (modified after Itasca, 2016).

In the PFC, macro parameters cannot be used directly in the modeling and micro parameters of the contact models should be calibrated using the macro parameter values. Therefore, the calibration is one of the most important parts of modeling with PFC (Yang et al., 2015; Mehranpour and Kulatilake, 2016). Since the SJCM is a relatively new model, limited effort has been made to find the effect of SJCM micro parameters on PFC modeling. This paper addresses and solves some of the shortcomings of the SJCM by improving micro parameters of SJCM and PFC methodology in using SJCM in modeling.

2. MODIFIED SMOOTH-JOINT CONTACT MODEL

The SJCM provides the linear elastic behavior in the normal and shear directions by specifying a constant value for joint normal stiffness, $k_n{}^J$, and a constant value for joint shear stiffness, $k_s{}^J$, along the contact line. The SJCM can be bonded or unbonded to model the cohesive or non-cohesive joints, respectively. For the unbonded SJCM, the maximum shear force is limited by imposing the Coulomb criterion with the friction coefficient of μ^J. However, for the bonded SJCM, this model provides the linear elastic behavior with the tensile strength cap ($\sigma_c{}^J$), and the shear strength cap ($\tau_c{}^J$). The shear strength can vary according to the Mohr-Coulomb failure criterion by specifying the cohesion, c^J, and friction angle, φ^J. When the bond breaks, the bonded SJCM changes to the unbonded SJCM (Itasca, 2016).

The slope of the joint normal stress versus the joint normal displacement diagram is known as the joint normal stiffness. Therefore, for modeling of joints in PFC, by defining a constant value for the normal stiffness of SJCM, this diagram shows the linear behavior with a constant slope angle. However, it contradicts the experimental evidences. Several researches emphasized on the non-linear behavior of this diagram and showed the joint normal stiffness varies with the normal stress acting on the joint surfaces. They provided different relations to model this behavior (Goodman, 1976; Bandis et al. 1983; Swan, 1983; Malama and Kulatilake, 2003; Kulatilake et al. 2016).

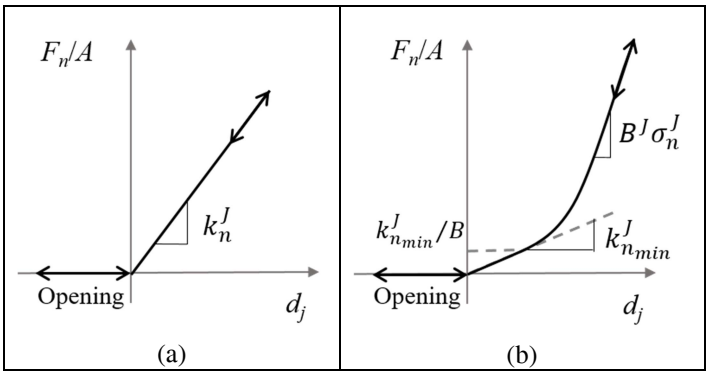

Fig. 2. Normal stress - normal displacement law for (a) SJCM and (b) MSJCM with equation 3.

Kulatilake et al. (2016) showed that the exponential function with the following equation can fit the experimental data properly. In this equation σ is the normal compressive stress, D_j is the joint normal displacement and A and B are the empirical constants that can be determined by performing regression analysis on the experimental test data.

$$\sigma = Ae^{BD_j} \quad (1)$$

They showed that when the natural logarithm is applied on both sides of equation 1, and then the resulting new equation is differentiated with respect to σ, the joint normal stiffness (K_n) results in a linear relation with the normal stress as given by the following equation.

$$K_n = \frac{\partial \sigma}{\partial D_j} = B\sigma \quad (2)$$

This equation can be used to modify $k_n{}^J$ in SJCM to have a non-linear model. Equation 3 shows the implemented algorithm in the Modified Smooth-Joint Contact Model (MSJCM). Because in the PFC it is impossible to have zero value for $k_n{}^J$, a minimum value of $k_{n_{min}}^J$ is set in this equation.

$$k_n^J = \max(k_{n_{min}}^J, B^J \sigma_n^J) \quad (3)$$

Fig. 2 shows the normal stress-displacement law for SJCM and MSJCM with equations 3.

The effect of $k_{n_{min}}^J$ and B^J on the normal compressive stress versus the joint normal displacement diagram in MSJCM as well as the comparison of MSJCM with SJCM are shown in Fig. 3. This figure is obtained from the simulation of the uniaxial compression test with a horizontal joint using PFC^{2D}. It should be mentioned that because in the PFC, the unit of k_n^J is $\frac{N}{m^3}$, the unit of B should be $\frac{1}{m}$.

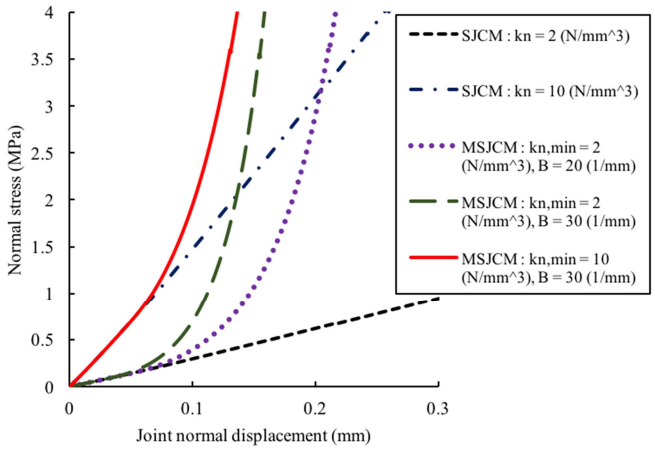

Fig. 3. Normal compressive stress versus joint normal displacement in PFC^{2D} modeling of the uniaxial compression test with a horizontal joint incorporating SJCM and MSJCM.

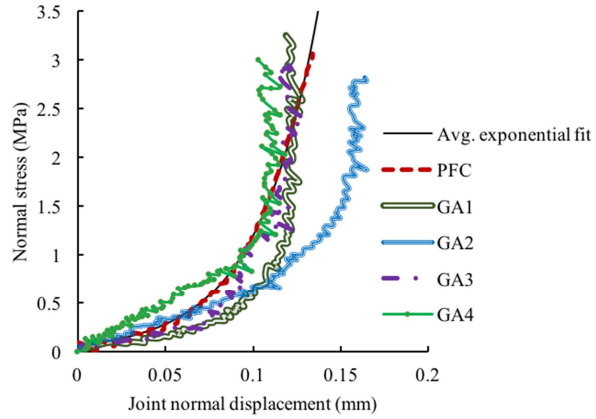

Fig. 4. Normal stress-joint normal deformation diagrams based on 4 experimental jointed uniaxial compression test results, the average exponential fit for normal stress-joint normal deformation relation, and PFC^{3D} modeling result based on MSJCM.

Fig. 4. Shows the experimental results of 4 uniaxial compression tests with a horizontal joint at the middle of the sample. These samples are synthetic and made out of a mixture of gypsum, sand, and water. They are cylindrical with 50 mm diameter, and the heights of 100 mm. This figure also shows the average exponential fit of equation 1 and calibrated numerical modeling result based on the MSJCM in the PFC^{3D}. This figure indicates the accuracy of the MSJCM in modeling the non-linear behavior of joint normal closure vs. normal stress. Table 1 shows the macro mechanical properties values of the synthetic samples and table 2 shows the calibrated micro mechanical properties based on the macro mechanical properties of table 1,

Table 1. Macro mechanical property values estimated for the synthetic intact rock and the joint from the laboratory test results

Intact rock		Joint	
Young's modulus (GPa)	1.07	Shear stiffness (GPa/m)	0.59
Uniaxial compressive strength (MPa)	5.57	B (1/mm)	28.9
Angle of internal friction (deg.)	23	Joint friction angle (deg.)	27.5

Table 2. Calibrated micro mechanical parameter values of the LPBM and MSJCM for the synthetic intact rock and joint in the PFC^{3D}

Intact rock	Joint
D_{min}= 2.7 mm m_r= D_{Max}/D_{min}= 1.66 E_c=$\bar{E}_c$= 1.2 GPa k_r=$\bar{k}_r$= 2.5 μ= 0.55 mean $\bar{\sigma}_c$= mean $\bar{\tau}_s$= 3.9 MPa std. dev. $\bar{\sigma}_c$= std. dev. $\bar{\tau}_s$= 0.975 MPa	μ^J= 0.5 k_s^J= 1.0 GPa/m k_n^J= 4.0 GPa/m B^J= 31.0 1/mm

3. INTERLOCKING PROBLEM

This problem was first reported by Bahaaddini et al. (2013) when they modeled the direct shear test in the PFC^{2D} using SJCM. They found that the shear strength suddenly increases when the joint displacement exceeds a value around the minimum particle diameter. They related this problem to the lack of a procedure in the PFC in creating new smooth-joint contacts. In order to explain this problem better, first the procedure in the PFC in assigning and updating the SJCM to contacts is explained as follows.

In the PFC the smooth-joint contacts are generally created in the bonded particle assembly by replacing those bonded contacts for which the lines connecting the centers of the adjacent particles intersect the intended joint plane after assembling the particles and before model execution. Thus, for example in the direct shear test modeling, the sample divides into two separate parts (Fig. 5a). The bonded part which is located above the joint is named: the upper bonded part; and the other bonded part which is located below the joint is named: the lower bonded part. The contact between each particle

from one part with any particles from the other part must be a smooth-joint contact.

Implementation of this condition becomes challenging when new contacts are created between these two groups because particles slide along the joint during the model execution. The PFC uses the same procedure as the one that is used in assigning SJCM at the first time. This means if a new contact occurs during the execution of the model and the line connecting the centers of the two particles intersects the intended joint line, this contact is set as a smooth-joint contact. Otherwise, it is set as a linear contact as a default. However, this procedure is not sufficient.

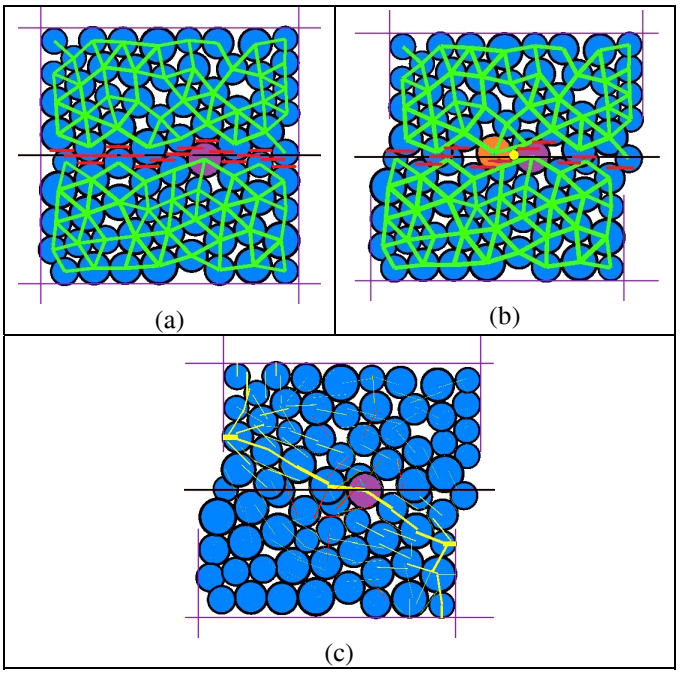

Fig. 5. (a) The created upper and lower bonded parts after applying a intended joint plane; the interlocking particle is shown in purple color, and the center of it is located beneath the intended joint plane, and belongs to the lower bonded part; (b) the created new linear contact due to the center of the purple ball crossing the intended joint plane after applying the normal, and shear stresses (green lines represent bonded contacts, red lines show the smooth-joint contacts, and the yellow dot shows the linear contact); (c) the stress concentration on the interlocking particle (yellow lines represent compressive forces, and red lines represent tensile forces).

For example, during the direct shear test, due to the normal and shear stresses, it is possible for a particle that belongs to either the upper or the lower bonded parts to cross the intended joint plane and to get located in the opposite side of the intended joint plane. Then, because of sliding, it is possible for this particle to have a new contact with a particle belonging to the opposite bonded part. Since these two particles are now located in the same side of the intended joint plane and their line connecting the two particle centers does not intersect the intended joint plane, their new contact is a linear contact instead of being a smooth-joint contact (Fig. 5b). In this situation, the aforementioned two particles cannot slide on each other parallel to the intended joint plane and they should slide perpendicular to their line connecting the two particle centers on their perimeters. Moreover, the defined normal stiffness and shear stiffness for the LCM are generally much higher compared to that of the SJCM. Consequently, these particles give rise to a rigid asperity on the joint surface. In this situation, the stress concentrates around this contact (Fig. 5c) and the shear strength increases. Bahaaddini et al. (2013) called the particle which crosses the intended joint plane as the "interlocking particle".

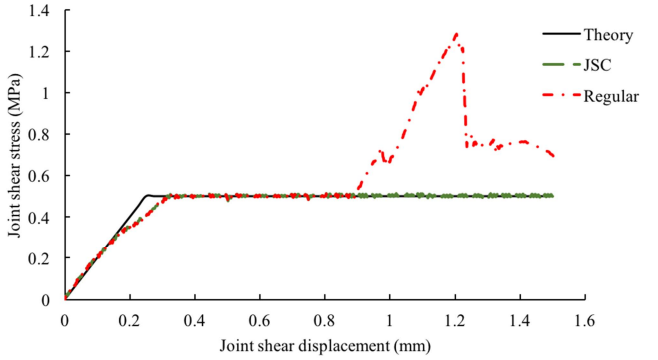

Fig. 6. shear stress versus shear displacement results for the direct shear test on a saw cut joint with a normal stress of 1 MPa using PFC^{2D} (the minimum, and maximum particle diameters were 1 mm, and 1.5 mm, respectively; the LPBM was chosen for modeling of the intact rock with mean tensile, and shear strengths of 5 MPa, and standard deviations of 1 MPa, a friction coefficient of 0.5, and a Young's modules of 1.2 GPa; for the SJCM, a normal stiffness of 10 GPa/m, a shear stiffness of 2 GPa/m, and a friction coefficient of 0.5 were chosen).

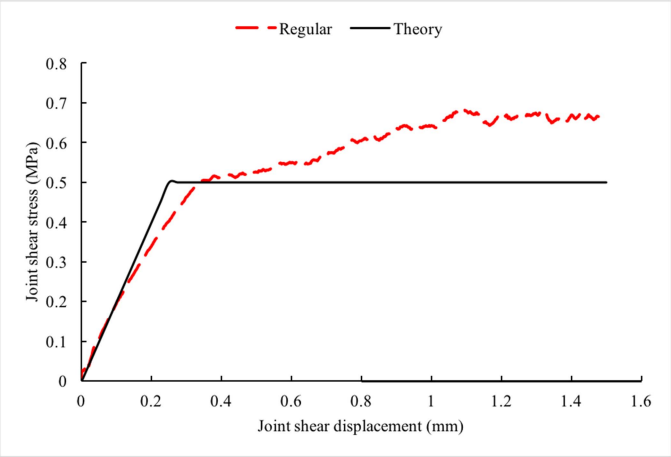

Fig. 7. shear stress versus shear displacement results for the direct shear test on a saw cut joint with a normal stress of 1 MPa using PFC^{3D} (sample dimension, particle properties and contact properties are the same as the properties in Fig. 6).

Fig. 6 shows increase of shear strength due to the interlocking problem in modeling with PFC^{2D}. In this

figure at the shear displacement of 0.9 mm, which is close to the minimum particle diameter (D_{min} = 1 mm), the interlocking occurs. However, in the PFC^{3D} model interlocking occurs at a lower shear displacement due to the spatial arrangement of the particles in 3-D. As an example, in Fig. 7, in the sample with the same properties as of the one in Fig. 6, the interlocking occurs around 0.35 mm (one third of the minimum particle diameter) in modeling with the PFC^{3D}. Nevertheless, the interlocking affects less on the shear strength of the joint in the PFC^{3D} compared to that of the PFC^{2D} because the spatial arrangement of the particles in 3-D leads to a lower dilation angle for the interlocking particles.

It should be also mentioned that, due to the force concentration around the interlocking particle, several unwanted bond failure occurs around this particle which can affect other mechanical behavior of the sample.

4. JOINT SIDES CHECKING APPROACH

In the previous direct shear tests, the interlocking happened when the centers of some particles are close to the intended joint plane. In this situation, with small displacements, the centers of these particles can cross the intended joint plane, and potentially make this problem. Besides, the intended joint plane in the PFC has a fixed position and in those direct shear tests like the one in Fig. 5, the normal and shear stresses are applied symmetrically and the joint is placed at the center of the sample. Therefore, the intended joint plane is always at the proper position. However, for an asymmetrical model due to the sample deformation during the model execution, the intended joint plane will not stay at the proper position. Thus, the expected value of the number of interlocking incidents increases. In order to solve the interlocking problem this paper proposes Joint Sides Checking approach (JSC).

In this approach, after applying the SJCM for the contacts around the intended joint plane like the one in the regular approach and before model execution, the particles with their centers located above the joint are marked as upside particles and the particles with their centers located beneath the joint are marked as downside particles (Fig. 8a). Then during the shear displacement, irrespective of the intended joint plane and the location of the centers of the particles, each new contact between the downside particles, and the upside particles is checked to be a smooth-joint contact; if a new non-smooth-joint contact is found, this contact is changed to a smooth-joint contact before the force displacement law applies on the new contact (Fig. 8b).

Fig. 8 shows that the particle and the new contact which made interlocking problem in Fig. 5, does not make any problem with the JSC. Fig. 6 also shows how well the new approach is matching with the theoretical result. With this method sample deformation cannot affect the joint plane since the intended joint plane does not play any role during the model execution and marked particles play the role to indicate the joint plane.

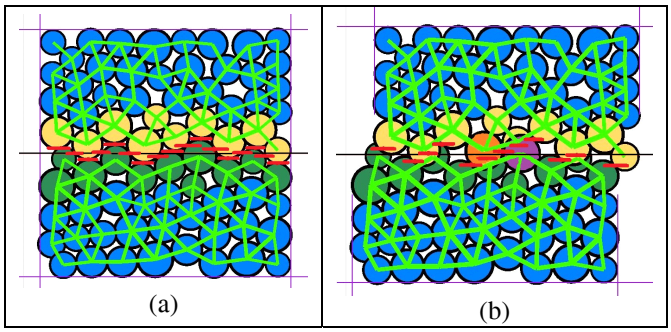

Fig. 8. Joint side checking approach: (a) marking of particles on the opposite sides of the intended joint plane [the upside (yellow), and the downside (green)]; (b) the new smooth-joint contact created between the purple particle from the downside group and the orange particle from the upside group.

Fig. 9 shows the bond failures in the direct shear test around the intended joint plane due to the shearing in Fig. 6. In the regular approach, the interlocking particles cause more cracks around themselves due to the force concentration around them. However, in the JSC approach only a few tensile cracks occur in some bonds around the intended joint plane which is normal in the direct shear test.

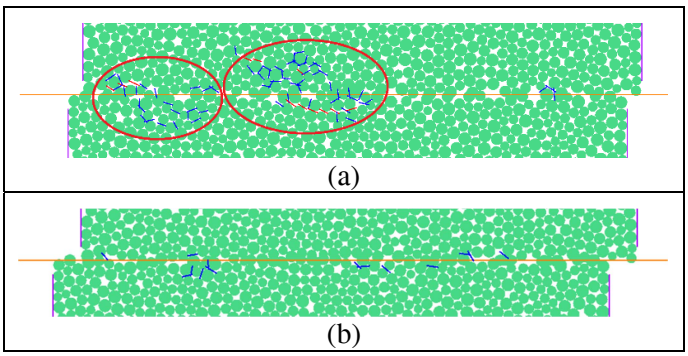

Fig. 9. Bond failures close to the intended joint plane in the (a) regular approach, (b) JSC approach (blue lines are the tensile bond failures, and red lines are the shear bond failures).

5. CONCLUSIONS

The SJCM currently available in the PFC code is a powerful tool to model the joint behavior in jointed rock masses. However, it has a few shortcomings. One of these shortcomings is the inability to capture the non-linear behavior of the joint closure due to changes in joint normal stress which leads to overestimation or underestimation of the joint closure value depending on the constant value of joint normal stiffness. This problem is solved in MSJCM by proposing the linear relation for the normal stiffness with the normal stress which is adopted from the experimental test. The comparison of the results between the experimental tests

and the numerical modeling showed the accuracy of MSJCM.

The other shortcoming is the interlocking problem which causes higher shear strength and a higher dilation angle for the joint. It also creates unwanted fractures around the intended joint plane. The effects of the interlocking problem on the shear strength and the dilation angle is much higher for the PFC^{2D} use compared to that of the PFC^{3D} use due to the spatial arrangement of the particles in three dimensions. However, this spatial arrangement leads to occurrence of the interlocking problem in PFC^{3D} at a lower ratio of the shear displacement to particle diameter compared to that in the PFC^{2D}. Besides, due to the higher number of particles around the intended joint plane in the PFC^{3D}, the possibility and the number of interlocking particles in the PFC^{3D} is higher. Therefore, the number of unwanted fractures around the intended joint plane is also higher in the PFC^{3D} use compared to that of the PFC^{2D} use.

The interlocking incident is dependent on the normal stress on the joint plane, the joint normal stiffness, the ratio of the particle size to the joint length and the ratio of the particle size to the shear displacement. The expected value of the number of interlocking incidents increases in response to several factors. These include cases with higher normal stress, lower joint normal stiffness, lower ratio of the particle size to the joint length and lower ratio of the particle size to the shear displacement.

The proposed approach, JSC, can properly solve the interlocking problem not only for the direct shear test but also for the other common tests in the rock mechanics field on jointed rock samples. This ability was shown for the direct shear test and the JSC approach results have agreed very well with the theory.

ACKNOWLEDGMENTS

The research was funded by the National Institute for Occupational Safety, and Health (NIOSH) of the Centers for Disease Control, and Prevention (Contract No. 200-2011-39886).

REFERENCES

1. Bahaaddini, M., Sharrock, G., Hebblewhite, B.K. 2013. Numerical direct shear tests to model the shear behaviour of rock joints. *Comput Geotech*. 51:101-115.
2. Bandis, S.C., Lumsden, A.C., Barton, N.R. 1983. Fundamentals of rock joint deformation. *Int J Rock Mech Min Sci Geomech.* 20(6):249–68.
3. Cundall P.A. 1971. A computer model for simulating progressive, large scale movements in blocky rock systems. *In: International symposium on rock mechanics,* Nancy, France: ISRM.
4. Cundall P.A. 1980. UDEC-A generalized distinct element pro- gram for modelling jointed rock. Report from P. Cundall Associates to U.S. Army European Research Office, London.
5. Cundall P.A. 1988. Formulation of a three-dimensional distinct element model—part I. A scheme to detect and represent contacts in a system composed of many polyhedral blocks. *Int J Rock Mech Sci Geomech.* 25:107–116.
6. Cundall P.A. and Strack, O.D. 1979. A discrete numerical model for granular assemblies. *Geotechnique* 29(1):47-65.
7. Goodman, R.E. 1976. Methods of geological engineering in discontinuous rocks. San Francisco: West Publishing Company.
8. Itasca Consulting Group Inc. 2016. PFC manual, version 5.0, Minneapolis.
9. Kulatilake, P.H.S.W., Shreedharan, S., Sherizadeh, T., Shu, B., Xing, Y., He, P. 2016. Laboratory estimation of rock joint stiffness and frictional parameters. *Geotech Geol Eng.* 34(6): 1723–1735.
10. Kulatilake, P.H.S.W., Shu, B. 2015. Prediction of rock mass deformations in three dimensions for a part of an open pit mine and comparison with field deformation monitoring data. *Geotech Geol Eng*. 33:1551-1568.
11. Kulatilake, P.H.S.W., Wang, S., Stephansson, O. 1993. Effect of finite size joints on deformability of jointed rock at the three dimensional level. *Int J Rock Mech Min Sci*. 30(5):479-501.
12. Malama, B., Kulatilake, P.H.S.W. 2003. Models for normal fracture deformation under compressive loading. *Int J Rock Mech Min Sci.* 40(6):893-901.
13. Mas Ivars, D., Pierce, M.E., Darcel, C., Reyes-Montes, J., Potyondy, D.O., Young, R.P., Cundall, P.A. 2011. The synthetic rock mass approach for jointed rock mass modelling. *Int J Rock Mech Min Sci*. 48(2):219-244.
14. Mehranpour, M.H., Kulatilake, P.H.S.W. 2016. Comparison of six major intact rock failure criteria using a particle flow approach under true-triaxial stress condition. *Geomech Geophy. Geo-energ Geo-resour*. 2(4):203-229
15. Potyondy, D.O. 2015. The bonded-particle model as a tool for rock mechanics research and application: current trends and future directions. *Geosyst Eng*. 18(1):1-28.
16. Potyondy, D.O., Cundall, P.A. 2004. A bonded-particle model for rock. *Int J Rock Mech Min Sci*. 41(8):1329-1364.
17. Shreedharan, S., Kulatilake, P.H.S.W. 2016. Discontinuum–equivalent continuum analysis of the stability of tunnels in a deep coal mine using the distinct element method. *Rock Mech Rock Eng*. 49(5):1903-1922.

18. Swan, G. 1983. Determination of stiffness and other joint properties from roughness measurements. *Rock Mech Rock Eng*. 16(1):19-38.

19. Wu Q., Kulatilake, P.H.S.W. 2012. REV and its properties on fracture system and mechanical properties, and an orthotropic constitutive model for a jointed rock mass in a dam site in China. *Comput Geotech.* 43:124-142.

20. Yang, X., Kulatilake, P.H.S.W., Jing, H., Yang, S. 2015. Numerical simulation of a jointed rock block mechanical behavior adjacent to an underground excavation and comparison with physical model test results. *Tunn Undergr Sp Tech.* 50:129-142.